

Adaptive Fuzzy High-order Sliding Mode Control for Flexible Air-breathing Hypersonic Vehicle

Junlong Gao, Ruyi Yuan and Jianqiang Yi

Institute of Automation, Chinese Academy of Sciences, Beijing, 100190, China

Junlong.gao@ia.ac.cn

Abstract - This paper proposes a multi-input multi-output (MIMO) adaptive fuzzy high-order sliding mode controller (FHOSMC) for the flexible air-breathing hypersonic vehicle (FAHV) longitudinal model. In order to suppress big uncertainties coming from flexible modes and make the system stably controlled, we design high-order sliding mode (HOSM) controller as the main controller to achieve system convergence in limit time, and adopt the fuzzy logic system (FLS) to generate adaptive parameters to adjust the control coefficients of HOSM controller online. In addition, tracking differentiator (TD) and nonlinear state observer (NSO) are designed to generate the high-order approximate commands and real-time derivatives of velocity and altitude respectively. The simulation results validate the effectiveness and robustness of the proposed controller.

Index Terms – *Flexible Air-breathing Hypersonic Vehicle, Fuzzy Logic System, FHOSMC, Nonlinear State Observer, Feedback linearization*

I. INTRODUCTION

Hypersonic vehicles have been widely researched since 1960s not only for being considered as a reliable and cost-effective way to access to space, but also because of the challenging tasks in materials, engines, control systems and so on. Forward work was basically focused on generic hypersonic flight vehicle (GHFV) [1], which is powered by rocket and made encouraging achievements in this field. A branch called air-breathing hypersonic vehicle (AHV) has been the hotspot in space research for recent decades. With the successful flight tests of X-43A and X-51A [2, 3], the wave-rider shape vehicle promoted more research work on AHV. However, special integrated configuration caused noticeable flexible modes and it cannot be neglected in control design. Therefore, a flexible air-breathing hypersonic vehicle (FAHV) model was introduced by Bolender and Donma which illustrated the fuselage flexibility effects as a free-free beam [4] so that the flexible modes and the coupling effects can be occurred through forces and moments [5].

Fuzzy set was introduced by Zadeh in 1965 [6] and after 9 years' effort, Mamdani successfully applied fuzzy set into control field [7]. Fuzzy logic system (FLS) and fuzzy logic control (FLC) are based on fuzzy sets which are more like human logic behavior to deal with high uncertain control issues. Sliding mode control (SMC) theory has the ability to drive system states (especially nonlinear systems) into a designed sliding surface and keeps the system robustly controlled. Fuzzy sliding mode control (FSMC) [8] which combined with FLC and SMC provides a simple way to

design the controller and makes the system asymptotically stable, which also contributes to reduce rules in FLC and still keeps system robustness when facing uncertainties. Moreover, Higher-order sliding modes (HOSM) inherit and develop main properties of the SMC and remove the restrictions including chattering effects and so on [9]. A Quasi-continuous HOSM theory has been applied to flexible air-breathing hypersonic vehicles to track the responses of the vehicle to a step change in velocity and altitude [10].

This paper proposes an adaptive fuzzy high-order sliding mode controller (FHOSMC) for FAHV. In order to deal with the noticeable vibration interferences coming from FAHV, we use high-order sliding mode controller (HOSMC) as the main controller to drive full state tracking errors to converge to zero in limit time and use fuzzy logic system to generate adaptive parameters which adjust control parameters in HOSMC online. The FHOSMC can make control system robust, which embodies in better command tracking performance and makes the elastic vibrations stably controlled.

II. PRELIMINARIES

A. FAHV Model Description

Assuming a flat Earth and normalizing the vehicle to unit depth, the nonlinear longitudinal dynamic motion equations of FAHV are given as [11]:

$$\dot{V} = (T \cos \alpha - D) / m - g \sin \gamma \quad (1)$$

$$\dot{\gamma} = (L + T \sin \alpha) / (mV) - g \cos \gamma \quad (2)$$

$$\dot{h} = V \sin \gamma \quad (3)$$

$$\dot{\alpha} = q - \dot{\gamma} \quad (4)$$

$$\dot{q} = M_{yy} / I_{yy} \quad (5)$$

$$\ddot{\eta}_i = -2\xi_i \omega_i \dot{\eta}_i - \omega_i^2 \eta_i + N_i, \quad i = 1, 2, 3 \quad (6)$$

This model is composed of eleven flight states:

$\mathbf{x} = [V, \gamma, h, \alpha, q]^T$ for rigid-body and $\boldsymbol{\eta} = [\eta_1, \dot{\eta}_1, \eta_2, \dot{\eta}_2, \eta_3, \dot{\eta}_3]$ for the first three flexible modes, which V, γ, h, α, q are the vehicle speed, flight path angle, altitude, angle of attack and pitch rate respectively. The nominal frequencies of the model are set as $\omega_1 = 21.17 \text{ rad/s}$, $\omega_2 = 53.92 \text{ rad/s}$ and $\omega_3 = 109.1 \text{ rad/s}$, while the damping ratio constant of flexible modes $\xi_i = 0.02$ includes severe mode vibration [12].

A control design model (CDM) to calculate approximated forces and moments is developed in [13]. The

forces and moments are described as:

$$\begin{cases} L \approx \frac{1}{2} \rho V^2 s C_L(\alpha, \delta, \eta) \\ D \approx \frac{1}{2} \rho V^2 s C_D(\alpha, \delta, \eta) \\ T \approx \frac{1}{2} \rho V^2 s [C_{T,\phi}(\alpha)\phi + C_T(\alpha) + C_T^\eta \eta] \\ M_{yy} \approx z_T T + \frac{1}{2} \rho V^2 s \bar{c} C_M(\alpha, \delta, \eta) \\ N_i \approx \frac{1}{2} \rho V^2 s [N_i^{\alpha^2} \alpha^2 + N_i^\alpha \alpha + N_i^{\delta_e} \delta_e + N_i^{\delta_c} \delta_c + N_i^0 + N_i^\eta \eta] \\ C_{T,\phi}(\alpha) = C_T^{\phi\alpha^3} \alpha^3 + C_T^{\phi\alpha^2} \alpha^2 + C_T^{\phi\alpha} \alpha + C_T^\phi \\ C_T(\alpha) = C_T^3 \alpha^3 + C_T^2 \alpha^2 + C_T^1 \alpha + C_T^0 \\ C_L(\alpha, \delta, \eta) = C_L^\alpha \alpha + C_L^{\delta_e} \delta_e + C_L^{\delta_c} \delta_c + C_L^0 + C_L^\eta \eta \\ C_D(\alpha, \delta, \eta) = C_D^{\alpha^2} \alpha^2 + C_D^\alpha \alpha + C_D^{\delta_e^2} \delta_e^2 + C_D^{\delta_c^2} \delta_c^2 + C_D^{\delta_e} \delta_e + C_D^{\delta_c} \delta_c + C_D^0 + C_D^\eta \eta \\ C_M(\alpha, \delta, \eta) = C_M^{\alpha^2} \alpha^2 + C_M^\alpha \alpha + C_M^{\delta_e} \delta_e + C_M^{\delta_c} \delta_c + C_M^0 + C_M^\eta \eta \\ C_j^\eta = [C_j^{\eta_1} \ 0 \ C_j^{\eta_2} \ 0 \ C_j^{\eta_3} \ 0], \quad j = T, L, D, M \\ N_i^\eta = [N_i^{\eta_1} \ 0 \ N_i^{\eta_2} \ 0 \ N_i^{\eta_3} \ 0], \quad i = 1, 2, 3 \end{cases} \quad (7)$$

where $\delta = [\delta_c, \delta_e]^T$, δ_c and δ_e are the deflection of canard and deflection of elevator respectively. Especially, the canard deflection gain k_{ec} is chosen a function relationship with elevator deflection [14] as $\delta_c = k_{ec} \delta_e$,

$$k_{ec} = -C_L^{\delta_e} / C_L^{\delta_c} \quad (9)$$

The air density ρ is defined as $\rho = \rho_0 \exp(-h/h_0)$ with $\rho_0 = 6.7429 \times 10^{-5} \text{ Slug} / \text{ft}^3$ and $h_0 = 24000 \text{ ft}$. A second-order engine model was introduced as:

$$\ddot{\phi} = -2\xi_n \omega_n \dot{\phi} - \omega_n^2 \phi + \omega_n^2 \phi \quad (10)$$

where ξ_n is the engine damping ratio, ω_n is the nominal engine frequency. ϕ is the throttle setting which ranges from 0.05 to 1.5. The output vector to be controlled is selected as $y = [V, h]^T$.

III. ADAPTIVE FUZZY HIGH-ORDER SLIDING MODE CONTROL DESIGN

We design an adaptive fuzzy high-order sliding mode controller (FHOSMC) for the flexible air-breathing hypersonic vehicle (FAHV) longitudinal model which has huge self-interference from flexible-mode vibrations and difficult to control. Moreover, we use step signals to verify the robustness and effectiveness of the controller. The FHOSMC combines fuzzy logic system (FLS) with high-order sliding mode controller (HOSMC) to adjust the control parameters adaptively. In addition, command tracking differentiator (TD) is used to generate arranged transition process (ATP) signals

of $\begin{bmatrix} V_d, \dot{V}_d, \ddot{V}_d \end{bmatrix}^T$ and $\begin{bmatrix} h_d, \dot{h}_d, \ddot{h}_d, \dddot{h}_d \end{bmatrix}^T$. Through the subtraction with those signals from nonlinear state observer (NSO), we obtain full state tracking errors in velocity and altitude channels respectively. All the tracking errors are needed in both system's dynamic inversion process and HOSMC to calculate full state high-order differentials. The overall control system diagram can be seen in Fig. 1.

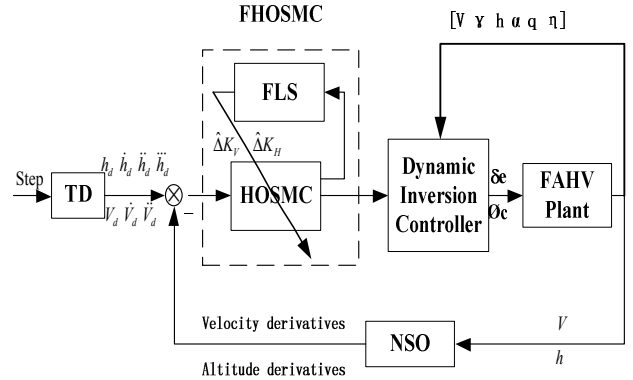


Fig.1 The block diagram of the overall control system

A. Sliding Mode Surface Design

In order to make the altitude h and velocity V track designed commands h_d and V_d , we select control vector as $u = [\delta_e, \phi_c]^T$ and define the following sliding mode surfaces based on desired tracking command:

$$s_1 = \sigma_V = e_v + \lambda_v \int_0^t e_v dt \quad (11)$$

$$s_2 = \sigma_H = e_h + \lambda_h \int_0^t e_h dt \quad (12)$$

where $e_v = V - V_d$, $e_h = h - h_d$ and λ_v , λ_h are strictly positive constants, the integrals of tracking errors can contributes to eliminate the steady state errors [10].

B. Feedback Linearization of FAHV

Based on differential geometric control theory, if the sums of linearized relative degrees r_i in each output y_i equal to the same order of the system, then the nonlinear system can be completely linearized [15]. Differentiating σ_V and σ_H three times and four times respectively, we obtain the following expressions:

$$\ddot{\sigma}_V = g_V - \dot{V}_d + \lambda_v \ddot{e}_v + T_{11} \delta_e + T_{12} \phi_c \quad (13)$$

$$\sigma_H^{(4)} = g_h - h_d^{(4)} + \lambda_h \ddot{e}_h + T_{21} \delta_e + T_{22} \phi_c \quad (14)$$

where

$$g_V = (\omega_1 \cdot \ddot{x}_0 + \dot{x}^T \cdot \Omega_2 \cdot \dot{x}) / m \quad (15)$$

$$g_h = 3\ddot{V} \cdot \dot{\gamma} \cdot \cos \gamma - 3V \cdot \dot{\gamma}^2 \cdot \sin \gamma + 3\dot{V} \cdot \ddot{\gamma} \cdot \cos \gamma - 3V \cdot \dot{\gamma} \cdot \ddot{\gamma} \cdot \sin \gamma$$

$$-V \cdot \dot{\gamma}^3 \cdot \cos \gamma + (\omega_1 \cdot \ddot{x}_0 + \dot{x}^T \cdot \Omega_2 \cdot \dot{x}) \cdot \sin \gamma / m \quad (16)$$

$$+ V \cdot (\pi_1 \cdot \ddot{x}_0 + \dot{x}^T \cdot \Pi_2 \cdot \dot{x}) \cdot \cos \gamma$$

$$T_{11} = \left(\frac{c_e \rho V^2 Sc}{2m \cdot I_{yy}} \right) \left(C_M^{\delta_e} - \frac{C_L^{\delta_e} C_M^{\delta_e}}{C_L^{\delta_e}} \right) \\ \left(\frac{\partial T}{\partial \alpha} \cos \alpha - T \cdot \sin \alpha - \frac{\partial D}{\partial \alpha} \right) \quad (17)$$

$$T_{12} = \frac{\omega^2}{m} \cdot \frac{\partial T}{\partial \phi} \cdot \cos \alpha \quad (18)$$

$$T_{21} = \left(\frac{\rho V^2 Sc}{2m I_{yy}} \right) \left(C_M^{\delta_e} - \frac{C_L^{\delta_e} C_M^{\delta_e}}{C_L^{\delta_e}} \right) \\ \left[\cos \gamma \left(\frac{\partial T}{\partial \alpha} \sin \alpha + T \cos \alpha + \frac{\partial L}{\partial \alpha} \right) \right. \\ \left. + c_e \sin \gamma \left(\frac{\partial T}{\partial \alpha} \cos \alpha - T \sin \alpha - \frac{\partial D}{\partial \alpha} \right) \right] \quad (19)$$

$$T_{22} = \frac{\omega^2}{m} \cdot \frac{\partial T}{\partial \phi} \cdot \sin(\alpha + \gamma) \quad (20)$$

with $\mathbf{x} = [V \ \gamma \ \alpha \ \phi \ h]^T$ and $\ddot{\mathbf{x}}_0 = [\ddot{V} \ \ddot{\gamma} \ \ddot{\alpha}_0 \ \ddot{\phi}_0 \ \ddot{h}]^T$. Then (13) and (14) can be written as:

$$\begin{bmatrix} \ddot{\sigma}_v \\ \sigma_h^{(4)} \end{bmatrix} = \begin{bmatrix} Y_1 \\ Y_2 \end{bmatrix} + T \cdot \mathbf{u} \quad (21)$$

where

$$T = \begin{bmatrix} T_{11} & T_{12} \\ T_{21} & T_{22} \end{bmatrix}, \quad \begin{bmatrix} Y_1 \\ Y_2 \end{bmatrix} = \begin{bmatrix} g_v - \ddot{V}_d + \lambda_v \ddot{e}_v \\ g_h - h_d^{(4)} + \lambda_h \ddot{e}_h \end{bmatrix}$$

According to (21) and using dynamic inversion control theory, the control vector can be designed as:

$$\mathbf{u} = \begin{bmatrix} \delta_e \\ \phi_c \end{bmatrix} = T^{-1} \begin{bmatrix} -Y_1 + \ddot{\sigma}_v \\ -Y_2 + \sigma_h^{(4)} \end{bmatrix} \quad (22)$$

However, due to the parameters $\ddot{\sigma}_v$ and $\sigma_h^{(4)}$ are hard to evaluate or calculate, there should be estimates to take places of $\ddot{\sigma}_v$ and $\sigma_h^{(4)}$.

C. Fuzzy High-order Sliding Mode Controller Design

Based on the high-order sliding mode (HOSM) control theory [9], we choose high-order sliding mode controllers G_v and G_h which are designed separately for their differences of relative degrees r_v and r_h . Then (22) can be written as:

$$\begin{bmatrix} \delta_e \\ \phi_c \end{bmatrix} = T^{-1} \begin{bmatrix} -Y_1 + G_v \\ -Y_2 + G_h \end{bmatrix} \quad (23)$$

where

$$G_v = -K_v \left(\ddot{\sigma}_v + \beta_1 \left(|\dot{\sigma}_v|^3 + |\sigma_v|^2 \right)^{1/6} g_{v2} \right) \quad (24)$$

$$G_h = -K_h \left\{ \ddot{\sigma}_h + \beta_2 \left[(\dot{\sigma}_h)^6 + (\dot{\sigma}_h)^4 + |\sigma_h|^3 \right]^{1/12} \cdot g_{h3} \right\} \quad (25)$$

$$\begin{cases} g_{v1} = \text{sat}(\sigma_v / \Phi_{v1}) \\ g_{v2} = \text{sat} \left[\left(\dot{\sigma}_v + |\sigma_v|^{2/3} \right) g_{v1} / \Phi_{v2} \right] \\ g_{h1} = \text{sat}(\sigma_h / \Phi_{h1}) \\ g_{h2} = \text{sat} \left[\left(\dot{\sigma}_h + 0.5 |\sigma_h|^{3/4} \cdot g_{h1} \right) / \Phi_{h2} \right] \\ g_{h3} = \text{sat} \left\{ \left[\ddot{\sigma}_h + \left((\dot{\sigma}_h)^4 + |\sigma_h|^3 \right)^{1/6} \cdot g_{h2} \right] / \Phi_{h3} \right\} \end{cases} \quad (26)$$

All the differentials can be calculated by (11) and (12). However, parameters $K_v, K_h > 0$ should be chosen strictly following $(\partial / \partial u)\sigma^{(r)} < 0$ to guarantee the control system *asymptotic stability*[9].

However, affected with the self-disturbance of flexible modes, the existing uncertainties of FAHV cannot be ignored. Therefore, parameters K_v and K_h should be adjusted online in order to enhance the robustness of the controller. Define K_v and K_h as:

$$K_v = K_{v0} + \hat{\Delta}K_v, \quad K_h = K_{h0} + \hat{\Delta}K_h \quad (27)$$

where $\hat{\Delta}K_v$ and $\hat{\Delta}K_h$ are adaptive parameters which are designed through fuzzy logic system, and K_{v0} and K_{h0} are their nominal values. These two terms can help K_v and K_h make the system controlled more quickly and more capable to adapt to variances under dynamic conditions.

The fuzzy rules for adaptive parameters consist of a collection of IF-THEN rules in the following forms:

For ΔK_v , Ruleⁱ : If x_1 is \widetilde{M}_1^i and x_2 is \widetilde{N}_1^i , then $\hat{\Delta}K_v$ is \widetilde{P}_1^i

For ΔK_h , Rule^j : If y_1 is \widetilde{M}_2^j and y_2 is \widetilde{N}_2^j , then $\hat{\Delta}K_h$ is \widetilde{P}_2^j

where i, j=1,2,...,5 is the number of rules. Based on preliminary knowledge we choose $x_1 = e_v$, $x_2 = \sigma_v \ddot{\sigma}_v$,

$y_1 = e_h$, $y_2 = \ddot{\sigma}_h$. \widetilde{M}_1^i , \widetilde{M}_2^j , \widetilde{N}_1^i , \widetilde{N}_2^j , \widetilde{P}_1^i and \widetilde{P}_2^j are all divided into {NB NS ZO PS PB}, where NB denotes “negative big”, NS denotes “negative small”, ZO denotes “zero”, PS denotes “positive small” and PB denotes “positive big”. The details of the fuzzy control rules are given in Table I and Table II. Input-output surfaces are shown in fig. 2.

TABLE I

$\hat{\Delta}K_v$ FUZZY RULES

$\sigma_v \ddot{\sigma}_v$	NB	NS	ZO	PS	PB
e_v					
NB	PB	PS	PS	PS	PB
NS	PM	PS	ZO	PS	PB
ZO	ZO	ZO	ZO	ZO	ZO
PS	PS	ZO	ZO	PS	PB
PB	PB	PS	ZO	PS	PB

TABLE II
 $\hat{\Delta}K_h$ FUZZY RULES

$\begin{array}{c} \hat{\sigma}_h \\ e_h \end{array}$	NB	NS	ZO	PS	PB
NB	PB	PS	PS	PS	PB
NS	PS	PS	ZO	PS	PS
ZO	PS	ZO	ZO	PS	PS
PS	PS	ZO	ZO	PS	PS
PB	PB	PS	PS	PS	PB

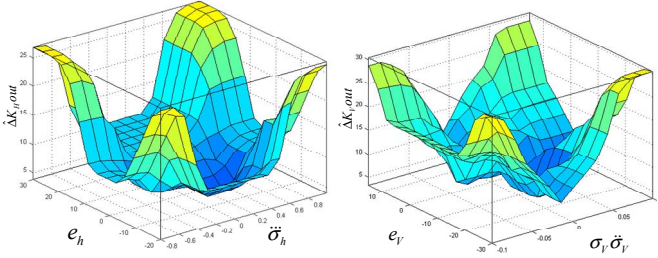


Fig.2 $\hat{\Delta}K_h$ and $\hat{\Delta}K_v$ fuzzy input-output surfaces

D. Tracking Differentiator Design

In the aforementioned controller, high-order derivatives of velocity and altitude are needed in both real and tracking commands. Being hard to obtained, this paper uses TD to process and to estimate derivatives of reference signals to form arranged tracking process.

Discrete TD algorithms are implemented as follows [16]: Velocity channel:

$$\begin{cases} fs_1(K) = -\lambda(\lambda(\lambda(v_{11}(K) - V_r) + 3v_{12}(K)) + 3v_{13}(K)) \\ v_{11}(K+1) = v_{11}(K) + \tau * v_{12}(K) \\ v_{12}(K+1) = v_{12}(K) + \tau * v_{13}(K) \\ v_{13}(K+1) = v_{13}(K) + \tau * fs_1(K) \end{cases} \quad (28)$$

Altitude channel:

$$\begin{cases} fs_2(K) = -\lambda(\lambda(\lambda(v_{21}(K) - h_r) + 4v_{22}(K)) + 6v_{23}(K)) + 4v_{24}(K) \\ v_{21}(K+1) = v_{21}(K) + \tau * v_{22}(K) \\ v_{22}(K+1) = v_{22}(K) + \tau * v_{23}(K) \\ v_{23}(K+1) = v_{23}(K) + \tau * v_{24}(K) \\ v_{24}(K+1) = v_{24}(K) + \tau * fs_2(K) \end{cases} \quad (29)$$

where λ is the “velocity factor” which can determine the speed of arranged process and τ is the “time step” which can decide the length of calculation step size. v_{11}, v_{12}, v_{13} represent $V_d, \dot{V}_d, \ddot{V}_d$ respectively, and $v_{21}, v_{22}, v_{23}, v_{24}$ represent $h_d, \dot{h}_d, \ddot{h}_d, \dddot{h}_d$ respectively. K is the number of iteration.

E. Nonlinear State Observer Design

We use NSO to estimate the exact flight states and their high derivatives online. Discrete NSO algorithms are implemented as follows [16]:

Velocity channel:

$$\begin{cases} e_1 = z_{11}(K) - V \\ z_{11}(K+1) = z_{11}(K) + \tau * (z_{12}(K) - \beta_{11} * e_1) \\ z_{12}(K+1) = z_{12}(K) + \tau * (z_{13}(K) - \beta_{12} * fal(e_1, 0.5, \tau)) \\ z_{13}(K+1) = z_{13}(K) + \tau * (-\beta_{13} * fal(e_1, 0.25, \tau) + U_1) \end{cases} \quad (30)$$

Altitude channel:

$$\begin{cases} e_2 = z_{21}(K) - h \\ z_{21}(K+1) = z_{21}(K) + \tau * (z_{22}(K) - \beta_{21} * e_2) \\ z_{22}(K+1) = z_{22}(K) + \tau * (z_{23}(K) - \beta_{22} * fal(e_2, 0.5, \tau)) \\ z_{23}(K+1) = z_{23}(K) + \tau * (z_{24}(K) - \beta_{23} * fal(e_2, 0.25, \tau)) \\ z_{24}(K+1) = z_{24}(K) + \tau * (-\beta_{24} * fal(e_2, 0.125, \tau) + U_2) \end{cases} \quad (31)$$

where $\beta_{11}, \beta_{12}, \beta_{13}$ and $\beta_{21}, \beta_{22}, \beta_{23}, \beta_{24}$ are the “tracking coefficients” which can decide observer performance and τ is the “time step” which decides the length of calculation step size. z_{11}, z_{12}, z_{13} represent V, \dot{V}, \ddot{V} and $z_{21}, z_{22}, z_{23}, z_{24}$ represent $h, \dot{h}, \ddot{h}, \dddot{h}$. $U_1 = T_{11}\delta_e + T_{12}\phi_c$ and $U_2 = T_{21}\delta_e + T_{22}\phi_c$.

IV. SIMULATIONS

The reference trajectories are set as 4000ft and 250ft/s step incremental commands in altitude and velocity command respectively. ATP parameters in velocity channel are set as $\tau = 0.01$, $\lambda = 0.8$ and in altitude channel are set as $\tau = 0.01$, $\lambda = 0.4$. FHOSMC parameters are chosen as $K_{V_0} = 40$, $K_{H_0} = 60$, $\beta_1 = 6$, $\beta_2 = 3$, $\lambda_v = 50$, $\lambda_h = 80$. NSO parameters are chosen as $\beta_{11} = 100$, $\beta_{12} = 300$, $\beta_{13} = 2000$, $\beta_{21} = 100$, $\beta_{22} = 300$, $\beta_{23} = 1000$, $\beta_{24} = 1800$, $k_{ec} = -0.79639$ and simulation time is 100s.

As shown in Fig. 3, both FHOSMC and HOSMC can track the ATP reference command in altitude channel with reasoning response. Fig. 4 shows that FHOSMC gets better altitude tracking performance than HOSMC, not only reducing the max value of tracking errors, but also making the tracking error converge more quickly.

Fig. 5 shows in velocity channel, both FHOSMC and HOSMC get reasonable response in 0-7s and 30-100s. In addition, Fig. 6 shows the max value of velocity tracking error is 17feet/s when using HOSMC, and the max value of velocity tracking errors 8.5feet/s when using FHOSMC. It is obviously that FHOSMC shows better velocity-command tracking performance than HOSMC.

Fig. 7 and Fig. 8 show the elevator deflection and throttle setting values. The HOSMC response is a little bit lagging behind FHOSMC.

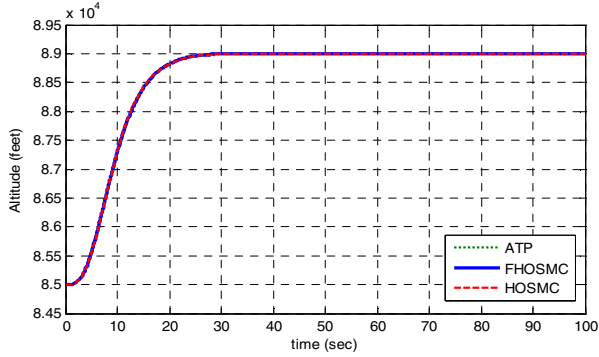


Fig.3 Response in altitude tracking

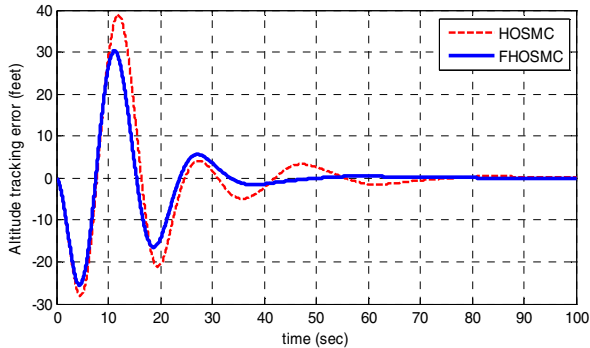


Fig.4 Altitude tracking errors

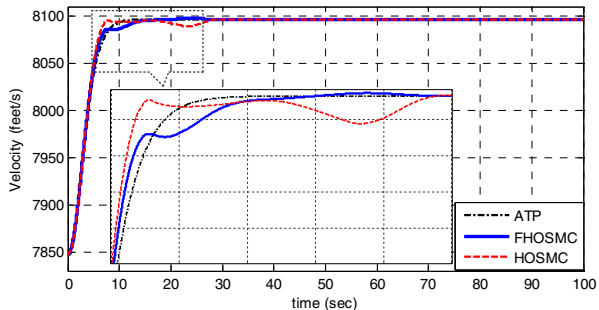


Fig.5 Response in velocity tracking

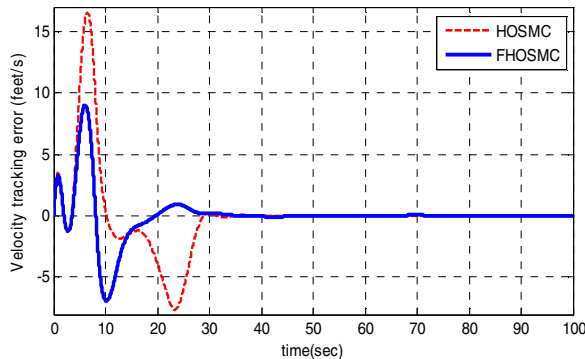


Fig.6 Velocity tracking errors

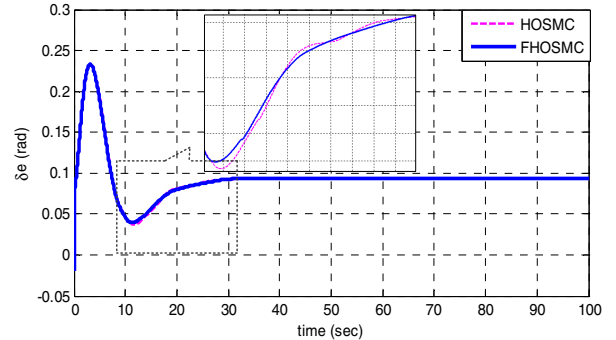


Fig.7 Elevator deflection

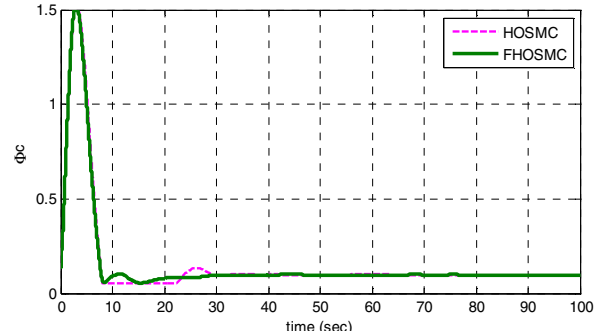


Fig.8 Throttle setting

Figs. 9-11 show FHOSMC and HOSMC both have strong ability to suppress vibration under three flexible modes. In first 5 seconds both the two controllers achieve to reduce the expand tendency of vibration and inhibit elastic modes stably in less than 40s. These three figures show strong robustness and high reliability of FHOSMC and HOSMC. However, by using FHOSMC we can get better responses of flexible mode rejections in Figs. 9-11.

Figs. 12-13 show the online adjusted values of parameters K_V and K_H in FHOSMC which contribute to better oscillation suppressions in control processes. Moreover, the zoom-in which shown in Fig. 5, Fig.7 and Figs. 9-11 validate the improvements respectively.

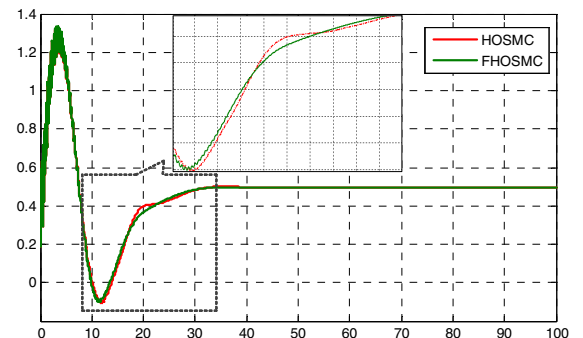


Fig.9 Response in flexible mode η_1

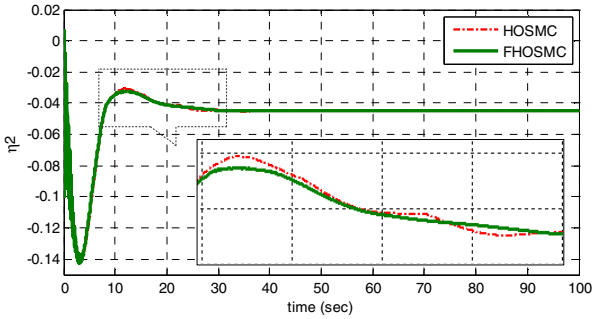


Fig.10 Response in flexible mode η_2

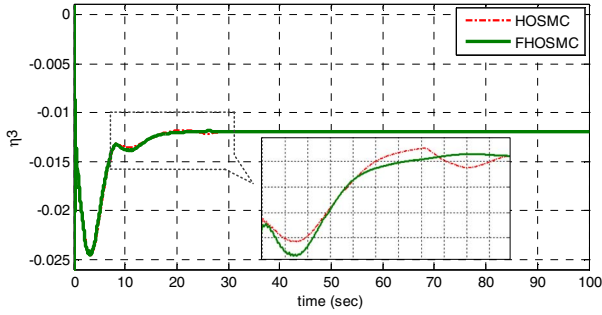


Fig.11 Response in flexible mode η_3

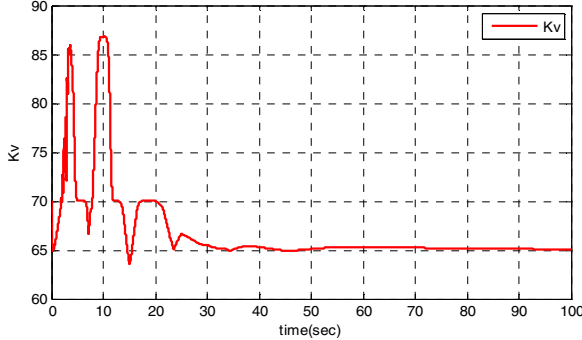


Fig.12 Value of online adjusted parameter K_v

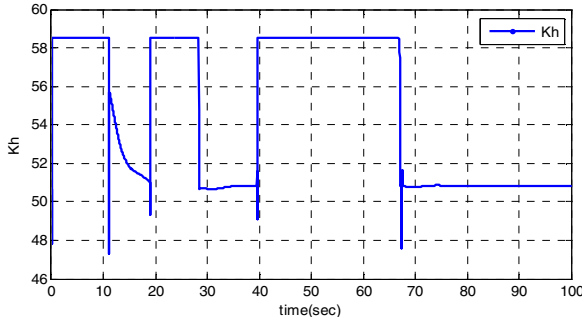


Fig.13 Value of online adjusted parameter K_h

V. CONCLUSION

This paper presents an adaptive fuzzy high-order sliding mode controller for a flexible air-breathing hypersonic vehicle. Tracking differentiator is designed to arrange tracking process commands and nonlinear state observer is designed to get real-time high-order differentials. Although it is hard to design

a robust controller due to the existing high nonlinearity, tight coupling and big uncertainties from FAHV longitudinal dynamics, high-order sliding mode controller (HOSMC) shows strong robustness and low chattering advantages. Moreover, the adaptive fuzzy high-order sliding mode controller (FHOSMC) can track the step command more effectively and can make the control system converge more quickly with lower cost in throttle settings and elevator deflection than HOSMC.

ACKNOWLEDGMENT

This work is supported by the grants of National Natural Science Foundation of China (No. 61273149, 61203003), and Innovation Methods of MOST No.2012IM010200.

REFERENCES

- [1] J. Shaughnessy, S. Pinckney, and J. McMinn, *Hypersonic vehicle simulation model: Winged-cone configuration*. NASA Technical Memorandum, 1990.
- [2] R. Voland, L. Huebner, and C. McClinton, "X-43A Hypersonic vehicle technology development," *Acta Astronautica*, vol. 59, pp. 181-191, 2006.
- [3] J. Hank, J. Murphy, and R. Mutzman, "The X-51A Scramjet Engine Flight Demonstration Program," in *15th AIAA International Space Planes and Hypersonic Systems and Technologies Conference*, 2008.
- [4] M. Bolender and D. Doman, "Nonlinear Longitudinal Dynamical Model of an Air-Breathing Hypersonic Vehicle," *Journal of Spacecraft and Rockets*, vol. 44, pp. 374-387, 2007.
- [5] L. Fiorentini, A. Serrani, M. Bolender, and D. Doman, "Nonlinear Robust Adaptive Control of Flexible Air-Breathing Hypersonic Vehicles," *Journal of Guidance, Control, and Dynamics*, vol. 32, pp. 402-417, 2009.
- [6] L. Zadeh, "Fuzzy Sets," *Information and Control*, vol. 8, pp. 338-353, 1965.
- [7] E. Mamdani, "Application of fuzzy algorithms for control of simple dynamic plant," in *Proceedings of the Institution of Electrical Engineers*, 1974, pp. 1585-1588.
- [8] C.-L. Chen and M.-H. Chang, "Optimal design of fuzzy sliding-mode control: A comparative study," *Fuzzy Sets and Systems*, vol. 93, pp. 37-48, 1998.
- [9] A. Levant, "Higher-order sliding modes, differentiation and output-feedback control," *International Journal of Control*, vol. 76, pp. 924-941, 2003.
- [10] Q. Zong, J. Wang, B. Tian, and Y. Tao, "Quasi-continuous high-order sliding mode controller and observer design for flexible hypersonic vehicle," *Aerospace Science and Technology*, vol. 27, pp. 127-137, 2013.
- [11] J. Parker, A. Serrani, S. Yurkovich, M. Bolender, and D. Doman, "Control-Oriented Modeling of an Air-Breathing Hypersonic Vehicle," *Journal of Guidance, Control, and Dynamics*, vol. 30, pp. 856-869, 2007.
- [12] D. Sighorsson, P. Jankovsky, A. Serrani, S. Yurkovich, M. Bolender, and D. B. Doman, "Robust Linear Output Feedback Control of an Airbreathing Hypersonic Vehicle," *Journal of Guidance, Control, and Dynamics*, vol. 31, pp. 1052-1066, 2008.
- [13] L. Fiorentini, "Nonlinear Adaptive Controller Design for Air-breathing Hypersonic Vehicles," Ph.D dissertation, The Ohio State University, Ohio, USA, 2010.
- [14] J. Parker, A. Serrani, S. Yurkovich, et al, "Approximate Feedback Linearization of an Air-breathing Hypersonic Vehicle," *AIAA Guidance, Navigation, and Control Conference and Exhibit*, August 2006.
- [15] H. Xu, M. Mirmirani, and P. Ioannou, "Adaptive sliding mode control design for a hypersonic flight vehicle," *Journal of Guidance, Control, and Dynamics*, vol. 27, no. 5, pp. 829-838, 2004.
- [16] J. Han, *Active Disturbance Rejection Control Technique*. Beijing: National Defense Industry Press, 2009.